Connectivity analysis of controlled quantum systems

Rong Wu, Herschel Rabitz, Gabriel Turinici, Ignatio Sola

Connectivity Analysis of Controlled Quantum Systems

Rong Wu and Herschel Rabitz*

Department of Chemistry, Princeton University, Princeton, NJ 08544

Gabriel Turinici

INRIA Rocquencourt, Domaine de Voluceau,

Rocquencourt B.P. 105, 78153 Le Chesnay Cedex, France†

Ignacio Solá

Departamento de Quimica Fisica I,

Universidad Complutense, 28040 Madrid (Spain)

(Dated: September 2, 2004)

Abstract

A connectivity analysis of controlled quantum systems assesses the feasibility of a field existing that can transfer at least some amplitude between any specified pair of states. Although Hamiltonians with special structure or symmetry may not produce full connectivity, it is argued and demonstrated that virtually any Hamiltonian is expected to be connected. The connectivity of any particular system is generally revealed in the quantum evolution over a single or at most a few time steps. A connectivity analysis is inexpensive to perform and it can also identify statistically significant intermediate states linking a specified initial and final state. These points are illustrated with several simple systems. The likelihood of an arbitrary system being connected implies that at least some product yield can be expected in the laboratory for virtually all systems subjected to a suitable control.

PACS numbers:

*Electronic address: hrabitz@princeton.edu

†CERMICS-ENPC, Champs sur Marne, 77455 Marne la Vallée Cedex, France

I. INTRODUCTION

Quantum control studies generally utilize a laser field for manipulating the system dynamics to achieve a desired physical objective, often consisting of maximizing the probability of transition between specified states of the system [1–4]. Many quantum optimal control simulations have produced excellent results, and increasing numbers of successful closed-loop learning control laboratory realizations are being reported [5–12]. Recent theoretical analysis [14, 15] revealed that the origin of these positive findings lies in there being no false sub-optimal search outcomes, provided that the system is controllable such that some field exists which may drive the amplitude from the initial to the final state. Underlying the concept of controllability is connectivity, which aims to establish that at least some pathway exists to connect the initial and final states. This paper presents the means to determine connectivity and then argues that virtually all quantum systems are expected to be connected. It will also be shown that a connectivity analysis can identify the intermediate states that are statistically likely to be more important in the dynamics. Section II defines the notion of quantum system connectivity and presents a very simple algorithm to test for its presence. Section III presents several simple illustrations, and some conclusions are drawn in Section IV.

II. CONNECTIVITY ANALYSIS

The quantum system under control is described by the Schrödinger equation:

$$i\hbar\frac{d|\psi(t)\rangle}{dt} = [H_0 - \mathcal{E}(t)\mu]|\psi(t)\rangle, \tag{1}$$

where $|\psi(t)\rangle$ is the time-dependent state of the system, H_0 is the field-free Hamiltonian, μ is the dipole moment, and $\mathcal{E}(t)$ is the laser control electric field. The quantum system is represented in terms of N basis states $\{|\psi_l\rangle\}$, $l = 1, 2, \ldots, N$, implying that $|\psi(t)\rangle$ is a vector of length N and correspondingly H_0 and μ are $N \times N$ matrices. The basis is conventionally chosen as the eigenstates of H_0, although any other basis may just as well be employed in the connectivity analysis. The connectivity analysis is in reference to the chosen basis. Section IV will generalize the analysis to other considerations of connectivity in controlled dynamics, including descriptions best formulated in coordinate space.

Two basis states $|\psi_i\rangle$ and $|\psi_j\rangle$ are said to be connected if some control field $\mathcal{E}(t)$, $0 < t \leq T$ exists creating a non-zero amplitude $U_{ji} = \langle\psi_j|U(T,0)|\psi_i\rangle$ relating the two states. Here $U(T,0)$ is the time evolution operator driven by the Hamiltonian $H_0 - \mathcal{E}(t)\mu$. The solution of the Schrödinger equation may be built up from a sequence of short time evolution operators $U(t, t-\Delta t)$,

$$U(t, t-\Delta t) \approx exp(-\frac{i\Delta t}{\hbar}[H_0 - \mathcal{E}(t - \frac{\Delta t}{2})\mu]) \tag{2}$$

for Δt being sufficiently small such that $\mathcal{E}(t)$ is nearly constant over $[t-\Delta t, t]$. Thus, the total propagation over the interval $0 < t \leq T$ may be carried out as follows [13]:

$$|\psi(T)\rangle \equiv U(T,0)|\psi_i\rangle = U(T, T-\Delta t) \times U(t-\Delta t, t-2\Delta t) \times \ldots \times U(\Delta t, 0)|\psi_i\rangle \ . \tag{3}$$

Two states $|\psi_i\rangle$ and $|\psi_j\rangle$ are connected if $|U_{ji}| \neq 0$, and the ultimate control goal is taken to be the maximization of $|U_{ji}|^2$. The maximum value of $|U_{ji}|^2$ generally builds up incrementally over the long sequence of the time evolution operations in Eq.(3). Yet, each incremental operator $U(t, t-\Delta t)$ contains similar physical coupling information with the only difference being the value $\mathcal{E}(\tau)$ involved. Except for the special case of $\mathcal{E}(\tau) = 0$, it is reasonable to expect that the basic assessment of connectivity resides in whether $|\langle\psi_j|U(t, t-\Delta t)|\psi_i\rangle| \neq 0$ for a value of $\mathcal{E}(\tau) \neq 0$ and $\Delta t \neq 0$. For numerical reasons, it is often prudent when performing a connectivity analysis with the operator in Eq.(2) to choose $\mathcal{E}(\tau)$ sufficiently large to assure that $||H_0|| \sim ||\mu|| \cdot |\mathcal{E}(\tau)|$ and also have Δt larger than normally required in the time integration steps of Eq.(3). The algorithm below for assessing connectivity also allows for the prospect that a product of two or more propagation steps may be needed to properly assess connectivity in cases when H_0 and μ have special structure or symmetry, but the numerical results from large ensembles of randomly chosen Hamiltonians supports the point that $U(t, t-\Delta t)$ alone usually reveals the system connectivity. The connectivity information is collected into a real symmetric matrix C whose elements C_{ji} are either 0 or 1, corresponding to whether state $|\psi_i\rangle$ and $|\psi_j\rangle$ are connected (i.e., $C_{ij} = 1$, if $|\psi_i\rangle$ and $|\psi_j\rangle$ are connected) by some non-zero amplitude. In some applications the connectivity of a particular pairs of states $|\psi_i\rangle$ and $|\psi_j\rangle$ is the focus, while in other cases the goal is to assess if $C_{ji} = 1$, for all $j < i$.

It is important to distinguish a connectivity analysis from performing a fully engaged optimal control calculation. The criterion $C_{ji} = 1$ is necessary for optimization, but $C_{ji} = 1$ does not guarantee that $|\langle\psi_j|U(T,0)|\psi_i\rangle| = 1$. This point will be evident in the simulations and the discussion in Section III. It is also important to distinguish a connectivity analysis from a controllability analysis, which aims to answer whether the control goal can be exactly met. Controllability is a strong requirement, while connectivity only asks if a non-zero amplitude exists between a pair of states. Thus, controllability implies connectivity, but connectivity does not guarantee controllability. Quantum controllability of U may be assessed using Lie Algebra techniques [16], which may be difficult to apply for systems of large dimension N. The strict assessment of 100% yield in the target state is often overly demanding for many applications where less than perfect control would still be acceptable. The connectivity analysis proposed in this paper is both conceptually and computationally simple while providing practically useful information.

The connectivity analysis is carried out with the following four algorithmic steps.

(i) Initialize the integer connectivity index K by setting $K = 1$.

(ii) Choose random constant field values $\mathcal{E}_k$, over a physically acceptable domain, $-\bar{\mathcal{E}} \leq \mathcal{E}_k \leq \bar{\mathcal{E}}$ and choose a set of random times $t_k > 0$, sampled on the interval $0 < t_k \leq T$, $k = 1, ..., K$.

(iii) Compute $\mathcal{U} = \prod_{k=1}^{K} exp[-i(H_0 - \mathcal{E}_k\mu)t_k/\hbar]$ and derive the K-th level connectivity map C^K by enumerating the non-zero elements of $\mathcal{U}$: $C^K_{ji} = 1$ if $|\mathcal{U}^K_{ji}| \neq 0$ and $C^K_{ji} = 0$ otherwise.

(iv) If all the elements of C are 1, then full connectivity is assured and one may exit the algorithm. If $C_{ji} = 1$ for a specified pairs of states for assessment, then again connectivity is assured between these two states and one may exit. If the portion of C^K of interest is not connected, then a further test may be performed by setting $K \to K + 1$ and returning to step (ii).

This algorithm builds on representation results of the dynamical Lie group of the system. This group, that determines all controllability properties, is shown [17] to be generated by all products in (iii) with arbitrary K.

For most cases, simply operating at $K = 1$ is sufficient to reliably assess connectivity. Considering $K = 1$, one may further expand $\mathcal{U}$ as follows:

$$exp[-\frac{i}{\hbar}(H_0 - \mathcal{E}_1\mu)t_1] = I + (H_0 - \mathcal{E}_1\mu)(-\frac{i}{\hbar}t_1) + \frac{1}{2!}(H_0 - \mathcal{E}_1\mu)^2(-\frac{i}{\hbar}t_1)^2 + \ldots \qquad (4)$$

As $\mathcal{E}_1$ and t_1 are random, we may conclude that $C^1_{ji} = 1$ as soon as at least one of the matrices $(H_0 - \mathcal{E}_1\mu)^l, l = 1, 2, \ldots,$ has an (j, i) matrix element whose magnitude is non-zero. By virtue of the Caley-Hamilton theorem [18], it suffices to check the matrices $(H_0 - \mathcal{E}_1\mu)^l$ for $l = 1, 2, \ldots, (N - 1)$. Finding connectivity by checking the matrices $(H_0 - \mathcal{E}_1\mu)^l$, $l = 1, 2, \ldots, (N - 1)$ for matrix elements of non-zero magnitude reveals the lowest order of l at which a connection between two states is first established. Furthermore, the statistics can be established for all intermediate states involved in the connected pathways at this level, which gives kinematic insight into the mechanism of the control. The statistical role of the intermediate states based on Eq.(4) may also be readily extended to $K > 1$, if necessary. In practice, the connectivity analysis is most conveniently carried out via the simple algorithmic steps (i)-(iv) above, and the further term-for-term assessment in Eq.(4) is only used if additional detailed kinematic coupling insight is sought.

III. ILLUSTRATIONS

In this section, the information revealed by a connectivity analysis and its ability to provide kinematic mechanism insights will be illustrated through three simple examples. The first example will make clear the distinction between connectivity and controllability. The second example will test connectivity for a large ensemble of randomly chosen Hamiltonians and examine the appropriateness of using just $K = 1$ in the analysis steps (i)-(iv). Finally, the last example will show that the connectivity analysis tools may be extended to multi-polarization fields and this case will also illustrate the extraction of kinematic mechanism information from Eq.(4).

A. Connectivity and controllability

Consider the four-level system as in Fig.1 where states 3 and 4 are degenerate. The field-free Hamiltonian H_0 of this system is assumed to have the diagonal form:

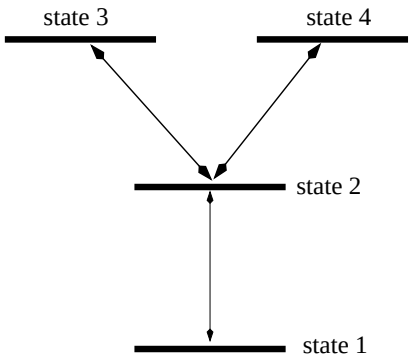

FIG. 1: The system used in example A.

$$H_0 = \begin{bmatrix} 1 & 0 & 0 & 0 \\ 0 & 2 & 0 & 0 \\ 0 & 0 & 3 & 0 \\ 0 & 0 & 0 & 3 \end{bmatrix}, \tag{5}$$

and the dipole matrix μ is chosen to be:

$$\mu = \begin{bmatrix} 1 & 1 & 0 & 0 \\ 1 & 1 & 1 & 1 \\ 0 & 1 & 1 & 0 \\ 0 & 1 & 0 & 1 \end{bmatrix} \tag{6}$$

The connectivity analysis in steps (i)-(iv) was complete at index $K = 1$, producing the connectivity matrix:

$$C = \begin{bmatrix} 1 & 1 & 1 & 1 \\ 1 & 1 & 1 & 1 \\ 1 & 1 & 1 & 1 \\ 1 & 1 & 1 & 1 \end{bmatrix} \tag{7}$$

The fact that all four states are mutually connected is immediately evident from a simple examination of Fig.1. However, this example was specifically chosen for illustration as the system is not fully controllable [16, 20]. The reason for this behavior is easily understood, as states 3 and 4 are degenerate and they are linked to state 2 by a transition dipole element of the same value. For example, if initially the population is in state 1, then no more than 50% of the population can be transferred to either state 3 or 4. However, if the symmetry is

broken by the slightest amount such that $|\mu_{32}| \neq |\mu_{42}|$, then the system remains connected and is now fully controllable.

B. Connectivity with arbitrary Hamiltonians and those with special structure

This section addresses the nature of connectivity likely to be found for arbitrary Hamiltonians as well as connectivity arising with Hamiltonians of special structure. In addition, the convergence of the algorithm in steps (i)-(iv) with respect to the index K will be demonstrated. First, a set of more than 10^4 random Hamiltonians H_0, μ of dimensions N up to 30 were examined by the algorithm. It was invariably found that the algorithm converged to a final matrix C at index $K = 1$, and furthermore all the cases were fully connected (i.e., $C_{ji} = 1$ for $\forall j, i$). These results demonstrate that the connectivity information is fully contained in an arbitrary incremental propagation step $U(t, t - \Delta t)$ for a random field value $\bar{\mathcal{E}} \neq 0$. Indeed, to find exceptions to this general behavior requires the creation of special cases. One special category occurs when H_0 and μ are increasingly sparse. Naturally, this circumstance can lead to some particular states being disconnected. But, in no case was $K > 1$ required to assess this matter when H_0 and μ are randomly chosen while containing some degree of imposed sparseness. Finally, the presence of special symmetries or extreme sparseness in H_0 and μ can lead to requiring $K > 1$ to achieve convergence. Specially engineered examples were found that required $K = 2$ to reveal the true converged connectivity matrix C. The need for $K > 1$ arises as the lack of commutation between $H_1 = H_0 - \mathcal{E}_1\mu$ and $H_2 = H_0 - \mathcal{E}_2\mu$ with $\mathcal{E}_1 \neq \mathcal{E}_2$ introduces the possibility of new linkages occurring for the case $\langle\psi_j|exp[-i(H_0 - \mathcal{E}_1\mu)\Delta t/\hbar]exp[-i(H_0 - \mathcal{E}_2\mu)\Delta t/\hbar]|\psi_i\rangle$ which does not show up in either $\langle\psi_j|exp[-i(H_0-\mathcal{E}_1\mu)\Delta t/\hbar]|\psi_i\rangle$ or $\langle\psi_j|exp[-i(H_0-\mathcal{E}_2\mu)\Delta t/\hbar]|\psi_i\rangle$. A similar argument would apply to the potential need for even higher K values.

The general conclusions from analyzing a large ensemble of random Hamiltonians are that (a) connectivity is easy to assess and (b) under most circumstances the connectivity is likely to be full, implying that at least some amplitude can be expected in the target state with a suitable field. Regarding the latter point, it was found that when considering sparse Hamiltonians, those of higher dimensions were generally more likely to exhibit full connectivity. These findings are illustrated by Fig.2, where the average fraction of connected states for Hamiltonians of different dimension N is plotted versus the probability p of any

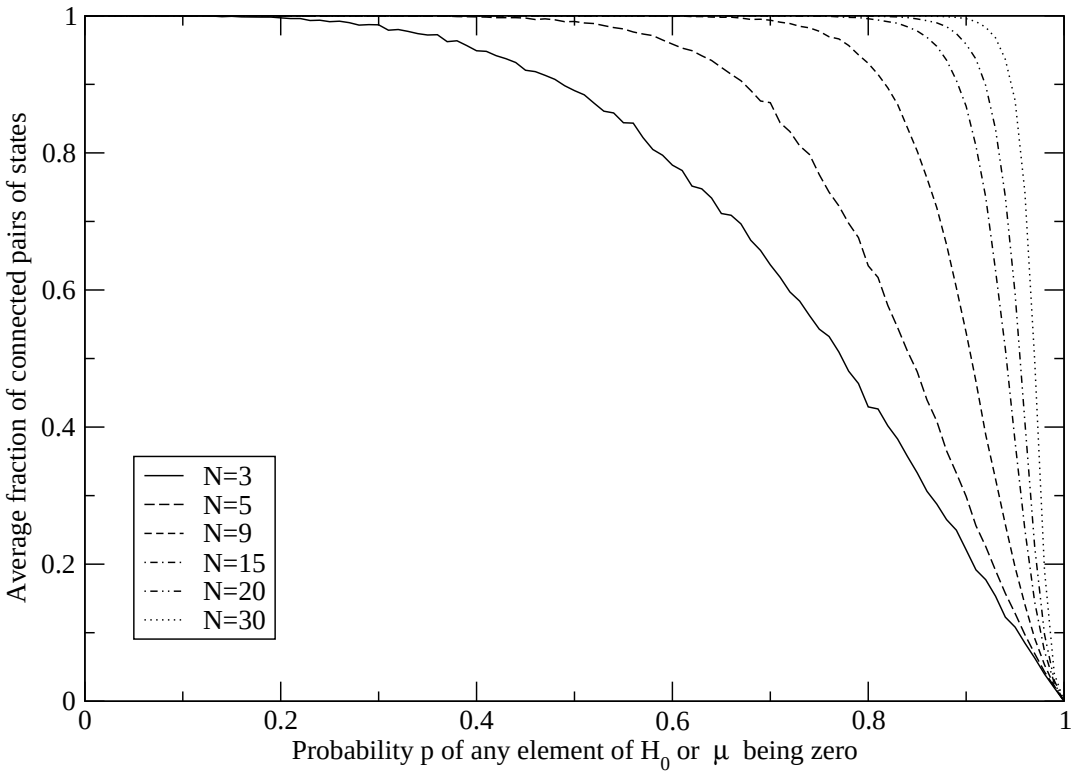

FIG. 2: The average fraction of connected pairs of states versus the probability p of any element of H_0 or μ being zero for Hamiltonian matrices of different dimension N.

element of the Hamiltonian matrices H_0 or μ being zero. For Hamiltonians of each dimension, the fraction of connected states is calculated by averaging the results from 20,000 runs, where the fraction at each run is the number of connected matrix elements in the upper triangular part of C divided by the total number of pairs of states $(N^2 - N)/2$. It can be seen from the figure that for increasing Hamiltonian sparseness (i.e., as the probability of any element of H_0 or μ being zero increases), the fraction of connected pairs of states initially is unaffected but eventually decreases. The clear trend shows that as the dimension N of the Hamiltonian matrices increases, the drop in the fraction of connected states is significantly delayed. A larger fraction of states on the average are connected for Hamiltonians of higher dimension, given the same degree of sparseness. This behavior evidently arises as the added states present with Hamiltonians of increasing dimension typically opens up new couplings that

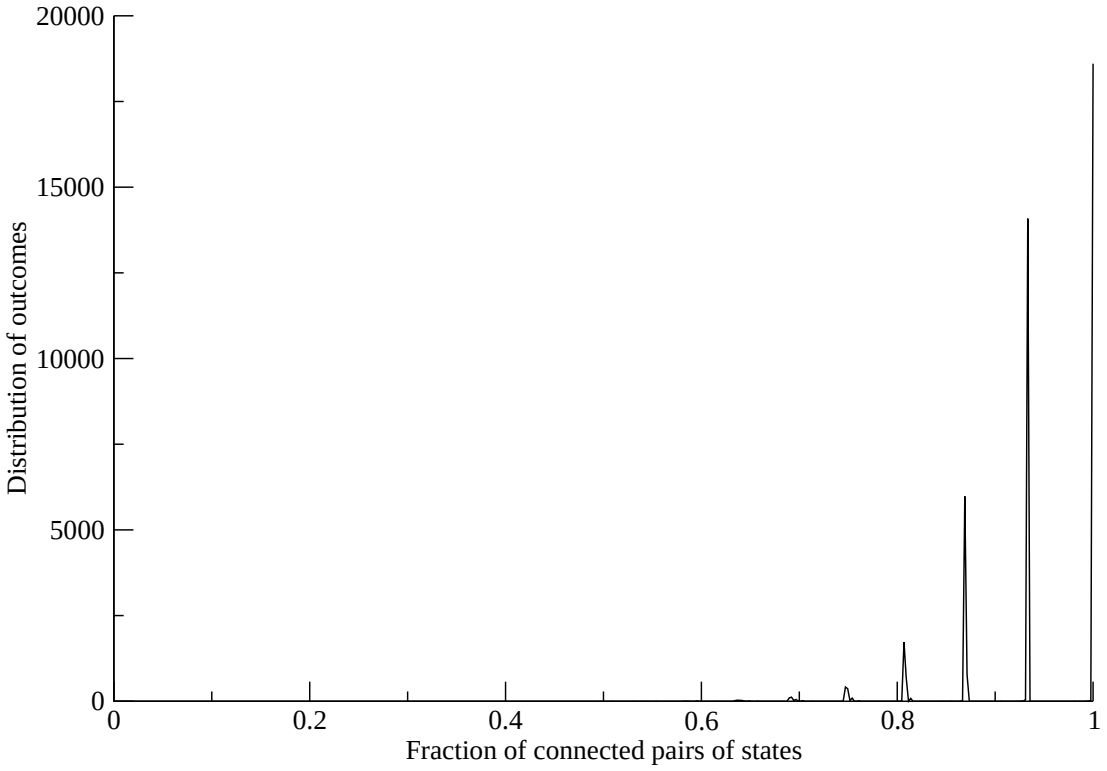

FIG. 3: The distribution of outcomes from 43,500 runs versus the fraction of connected pairs of states for a Hamiltonian of dimension $N = 30$ and probability $p = 0.94$ of any element of H_0 or μ being zero.

can overcome those that might be restricted in lower dimensional cases. Realistic physical systems typically have very large dimensions, and thus are expected to be fully connected in most cases. This latter point is also supported by a mathematical theorem in random graph theory [26]. In a random graph of N vertices the presence of an edge between any two vertices is assigned a probability p'. The random graph in turn can be represented by random matrices where the probability p' of the (i, j) matrix element being non-zero corresponds to the likelihood of there being an edge between vertex i and vertex j. The theorem states that there exists a threshold function $p'(N) = \frac{\ln N}{N^2}$ such that a random graph is *almost always*[28] connected when $p' \geq \frac{\ln N}{N^2}$. The Hamiltonian $H_0 - \mathcal{E}(t)\mu$ studied in this section is a linear combination of two independent Hermitian random matrices: H_0 and

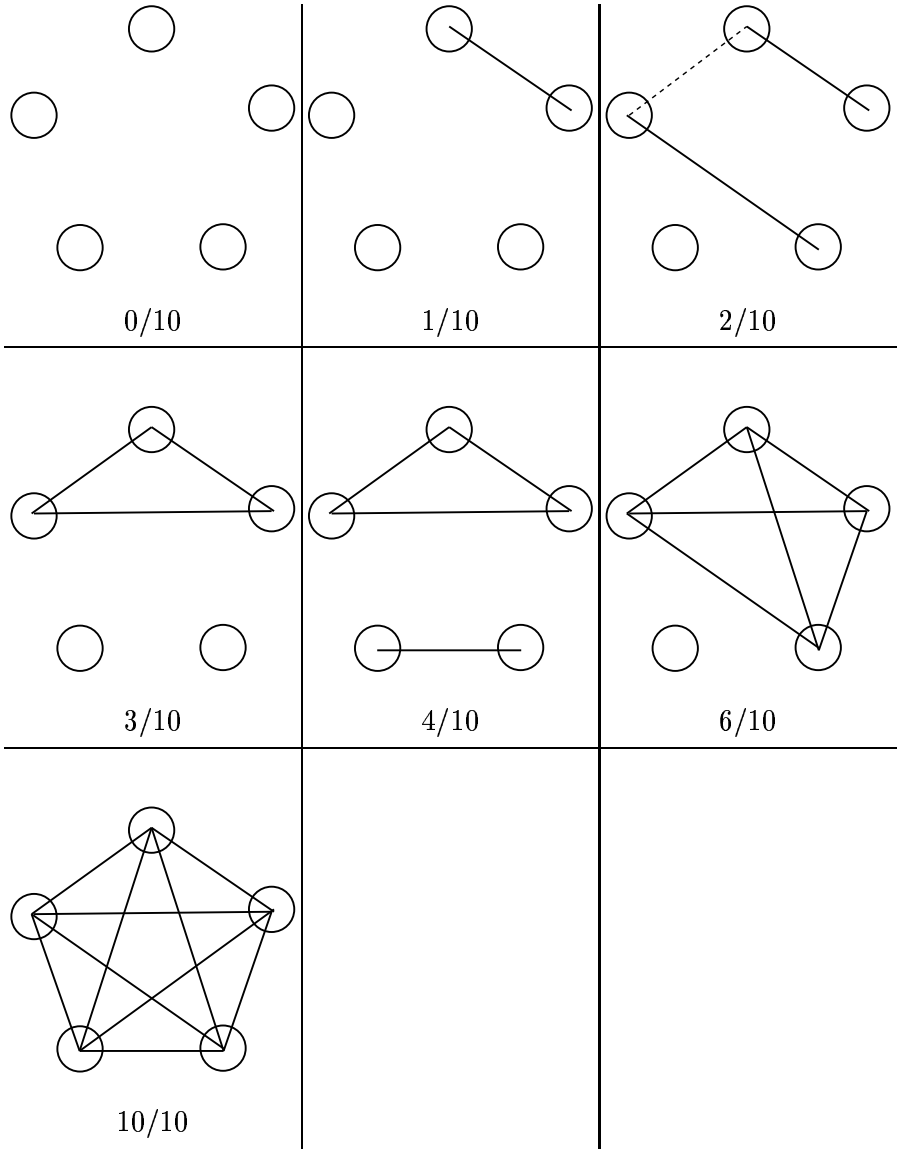

FIG. 4: All 7 possible connectivity pictures of a random graph with $N = 5$. Note that vertices i and k will be connected if vertex i connects to vertex j and vertex j connects to vertex k. For example, adding an edge at the position shown by the dashed line in the picture "2/10" would induce more connections and transform the picture into "6/10".

μ. The algorithm in steps (i)-(iv) operating at $K = 1$ (i.e., the expansion in Eq.(4) can be carried out) is equivalent to analyzing the connectivity of a graph represented by the matrix $H_0 - \mathcal{E}(t)\mu$, i.e., the resultant connectivity information of this graph is stored in the matrix C. Let p' be the probability of any matrix element of H_0 or μ being non-zero, $p' = 1-p$. The corresponding threshold function for the full connectivity of this Hamiltonian system as a graph is $p'(N) = \frac{\sqrt{\ln N}}{N}$. Expressed in terms of $p(N)$, the threshold function is:

$p(N) = 1 - \frac{\sqrt{\ln N}}{N}$. For $N = 30$, $p \sim 0.94$. That is, a connected system at $N = 30$ can tolerate approximately 94% zeroes in the matrices H_0 and μ. Larger N leads to better tolerance. Realistic physical systems typically have large dimension N and thus are expected to be fully connected. Figure 3 shows the statistical distribution of the connectivity outcomes from a simulation of 43,500 random Hamiltonians at $N = 30$ and $p = 0.94$. A majority of the Hamiltonians produce full connectivity, confirming the above graph theoretical prediction. The distribution is evidently *discrete*[29], and it was further observed that as the dimension N of the Hamiltonian increases, this discretization pattern becomes even sharper. This behavior implies that the connectivity of a physical system is 'quantized', which may be attributed to the inherent properties of random graphs. To understand this, consider a random graph with $N = 5$. The graph has a total of 10 pairs of vertices. Thus, there are 11 possible values for the fraction of connected pairs of vertices: 0/10, 1/10, ..., 9/10, 10/10. However, only 7 values among them are actually admissible: 0/10, 1/10, 2/10, 3/10, 4/10, 6/10 and 10/10, as shown in Fig.4. These are also all the possible outcomes of C computed by the algorithm in steps (i)-(iv) with random Hamiltonians of dimension $N = 5$. The discretization occurs in the range of high values of the fraction (i.e., the missing values are: 5/10, 7/10, 8/10 and 9/10). Intuitively, as the number of connected pairs rises, the graph becomes so intertwined that isolating unconnected pairs gradually becomes impossible; this point is illustrated in Fig.4 with the case of 2/10 where the addition of one particular connection led to 6/10. As N rises, it is expected that the graph will become even more entangled, and that an even wider range of values of the fraction will vanish, resulting in a highly discretized distribution pattern.

Although full connectivity does not assure full controllability, again it would take special structure or accidental values of the Hamiltonian matrix elements to forbid this from happening. In conclusion, it is expected that a null measured set of Hamiltonians will be either disconnected or uncontrollable. Those that violate this "rule" are likely to have special structure or symmetry, and a case related to this point is given in Section III C. The physical consequences of full connectivity and controllability likely being the rule will be discussed in Section IV.

C. Connectivity with multi-polarization fields

There is much interest in utilizing multi-polarization control fields to manipulate the dynamics of molecules containing special symmetries (e.g., the control of optical enantiomers [22–24]). As an illustration of the role of multi-polarization fields, consider the simple model system [25] of a three dimensional harmonic oscillator having a cubic coupling term (with $k_1 = 5 \times 10^{-5}$),

$$H_0 = \sum_{i=1,2,3} (\frac{p_i^2}{2} + \frac{\omega^2 q_i^2}{2}) + k_1 q_1 q_2 q_3 \ , \tag{8}$$

where the q_i's are the coordinates and p_i's the corresponding momenta, with the frequency $\omega = 0.02$. All variables are in atomic units. The coupling term models the presence of anharmonicity. We assume that the system is oriented such that the dipole moment components coincide with the polarization directions of the laser field. A simple model is also assumed with each dipole component μ_i varying linearly in q_i, such that

$$\vec{\mu} \cdot \vec{\mathcal{E}}(t) = k_2[q_1 \cdot \mathcal{E}_1(t) + q_2 \cdot \mathcal{E}_2(t) + q_3 \cdot \mathcal{E}_3(t)] \tag{9}$$

where $k_2 = 1.0 \times 10^{-2}$.

The Hamiltonian is represented in the first 84 harmonic oscillator eigenstates of $\sum_{i=1,2,3}(\frac{p_i^2}{2} + \frac{\omega^2 q_i^2}{2})$. There can be three different types of 1-D control pulses, each of which corresponds to one of the three polarization components $\mathcal{E}_1(t), \mathcal{E}_2(t)$ and $\mathcal{E}_3(t)$. For control with 2-D pulses, there can also be three different types of pulses, where each corresponds to a different combination of two polarization components. Together with the case of control using a full 3-D pulse, there are seven cases. The goal is to assess connectivity between the pair of states $|0,0,0\rangle$ and $|1,2,3\rangle$. This situation has component Hamiltonian matrices H_0 and μ_1, μ_2, μ_3 corresponding to the three dipole components. The constant fields $\mathcal{E}_1, \mathcal{E}_2$ and $\mathcal{E}_3$, were randomly chosen and a $K = 1$ level analysis gave a converged connectivity assessment. The connectivity results found from the algorithm are listed in Table I. For control with 1-D polarization fields, the selected target state is only accessible from the initial state (i.e., they are connected) by the second polarization component $\mathcal{E}_2(t)$. This case with the single fields $\mathcal{E}_1(t)$ or $\mathcal{E}_3(t)$ alone is an example of where the special symmetry in the Hamiltonian and the choice of initial and final states for assessment leads to disconnected situations. However, for controls with 2-D and 3-D polarization fields in this example, the target state

Case	Control	$\|0,0,0\rangle$ and $\|1,2,3\rangle$ connected?
1	$\mathcal{E}_1(t)$	No
2	$\mathcal{E}_2(t)$	Yes
3	$\mathcal{E}_3(t)$	No
4	$\mathcal{E}_1(t), \mathcal{E}_2(t)$	Yes
5	$\mathcal{E}_2(t), \mathcal{E}_3(t)$	Yes
6	$\mathcal{E}_1(t), \mathcal{E}_3(t)$	Yes
7	$\mathcal{E}_1(t), \mathcal{E}_2(t), \mathcal{E}_3(t)$	Yes

TABLE I: Connectivity results for the model in Example C

is always accessible, including with combined fields $\mathcal{E}_1$ and $\mathcal{E}_3$ where acting alone they did not connect the specified initial and final states. These results were also confirmed [25] with analogous optimal control calculations.

Based on the connectivity analysis using Eq.(4), a statistical count was also made on the number of times a particular intermediate state is involved in the shortest pathway connecting the initial state $|0,0,0\rangle$ to the target state $|1,2,3\rangle$ for simulation case 2 and cases 4 to 7 in Table I. The shortest connectivity linkage showed up with four intermediate states, and the statistical analysis is applied at this level. For cases 4 to 7, even at the level of four intermediate states, there were 189 kinematic pathways linking $|0,0,0\rangle$ to $|1,2,3\rangle$. A few intermediate states showed up consistently as playing central roles. Most important is state $|1,1,1\rangle$ which appeared twice as frequently as the next most visited states $|0,1,2\rangle, |1,2,1\rangle$ and $|2,1,2\rangle$. The plethora of potential control pathways offers rich opportunities for achieving excellent control outcomes, as confirmed by optimal control calculations [25]. A full mechanistic pathways analysis [21] would be required to reveal the actual amplitude associated with any possible connected pathway between the initial and final states.

IV. CONCLUSIONS

This paper presented a very simple algorithm for readily testing the connectivity of controlled quantum systems having a discrete set of N states. Some applications are inherently discretely represented (e.g., coupled spin systems), while others become so upon practical treatment. An example of the latter case was the coupled oscillator system in Eqs.(8) and

(9) which was naturally represented in a harmonic oscillator basis. However, this latter application and others could just well be represented in coordinate space which is discretized on some suitable grid. The connectivity analysis algorithm in steps (i)-(iv) could also be applied in this case. As noted in Section II, the connectivity analysis is performed in reference to a chosen basis, and special considerations arise regarding the basis used to assess connectivity in this situation. In the case of the coordinate space representation one perspective would correspond to the fine grained view of assessing if some arbitrary points r_i and r_j in the space are connected by the dynamics. However, this level of fine detail is likely more than required for many applications, and a reasonable assessment would consist of asking if any of the points in a local volume V_i are connected to any of the points in the local volume V_j. Here V_i and V_j could, for example, correspond to the configuration space volumes that contain the main portions of the initial wave packet and the target one, respectively. An associated reduced dimensional connectivity matrix C may be defined to focus on the connectivity of V_i and V_j or simultaneously with other sub-volumes in the configuration space. An analogous reduced dimensional connectivity matrix C concept could also be established for problems defined in terms of an eigenbasis, such as from H_0. Connectivity between one subset of states $\{\psi_i\}$ and another subset of states $\{\psi_j\}$ is natural to assess in many circumstances. For example, in some cases the control interest may lie in transfer from one electronic state to another, regardless of the underlying ro-vibrational states involved; here $\{\psi_i\}$ and $\{\psi_j\}$ would be the associated sets of two ro-vibrational states. The assessment of such reduced connectivity issues would operate with the same algorithmic steps (i)-(iv) presented in Section II, and a compression of the information into a reduced matrix C follows as an easy final step.

There is much interest in the mechanisms by which control fields achieve their action in any particular application. Recent work [21] has defined the control mechanism in terms of quantitatively identifying the significant multi-state pathway amplitudes linking the initial and final states $|\psi_i\rangle$ and $|\psi_j\rangle$. The contribution of any particular pathway can draw on delicate features of the control field. Nevertheless, connectivity is the basic criterion for any particular pathway playing a role. The connectivity analysis provides a simple way of identifying these kinematically allowed pathways. Importantly, those intermediate states that appear to have a key role can be easily found by a simple statistical analysis of their frequency of appearance in the family of pathways up to some specified order in Eq.(4). The

detailed dynamics driven by a particular optimal field will finally weigh in to determine the actual contributing pathways [21], but the simplicity of performing a connectivity assessment provides an easy way to attain an initial glimpse of what is taking place.

Finally a significant finding in this paper is the observation that virtually all Hamiltonians are expected to have fully connected dynamics. As commented earlier, establishing connectivity is a necessary criterion for a system to be controllable. Although full controllability may not be concluded from full connectivity, it is reasonable to expect that at least a high degree of controllability, if not full controllability, will exist in cases showing full connectivity. Furthermore, increasing system complexity in terms of many coupled states being present likely aids rather than hinders this situation. These points are especially relevant as a recent work [14] has shown that all controllable quantum systems only have perfect solutions for state-to-state population transfer under optimal control (i.e., there are no sub-optimal extrema).

One attraction of performing a connectivity analysis is the ease of its execution relative to the information that can be gained. Connectivity as a powerful tool is not confined to theoretical studies, and is playing into the laboratory control experiments. For example, an experiment reported a design for a quantum AND gate which was elegantly tested utilizing the connectivity of graphs [27]. It is anticipated that further insights will follow from applying connectivity assessments in additional quantum control circumstances.

Acknowledgments

R. Wu, H. Rabitz and I. Solá acknowledge support from the National Science Foundation and an ARO-MURI grant.

---

[1] S. Shi, A. Woody, H. Rabitz, J. Chem. Phys., 88, 6870-6883 (1988)

[2] R. Kosloff, S. A. Rice, P. Gaspard, S. Tersigni, and D. J. Tannor, Chem. Phys., 139, 201-220 (1989)

[3] S. Shi, H. Rabitz, Chem. Phys., 97, 276-287 (1992)

[4] I. Walmsley and H. Rabitz, Phys. Today, 56, 43-49 (2003)

[5] A. Assion, T. Baumert, M. Bergt, T. Brixner, B. Kiefer, V. Seyfried, M. Strehle, and G. Gerber, Science, 282, 919-922 (1998)

[6] T. Weinacht, J. Ahn, and P. Bucksbaum, Nature, 397, 233-235 (1999)

[7] R. Bartels, S. Backus, E. Zeek, L. Misoguti, G. Vdovin, I. Christov, M. Murnane, and H. Kapteyn, Nature, 406, 164-166 (2000)

[8] R. Levis, G. Menkir, and H. Rabitz, Science, 292, 709-713 (2001)

[9] T. Brixner, N. Damrauer, P. Niklaus, and G. Gerber, Nature, 414, 57-60 (2001)

[10] R. Bartels, T. Weinacht, S. Leone, H. Kapteyn, and M. Murnane, Phys. Rev. Lett., 88, 033001-1-033001-4 (2002)

[11] J. Herek, W. Wohlleben, R. Cogdell, D. Zeidler, and M. Motzkus, Nature, 417, 533-535 (2002)

[12] C. Daniel, J. Full, L. Gonzalez, C. Lupulescu, J. Manz, A. Merli, S. Vajda, and L. Woste, Science, 299, 536-539 (2003)

[13] F. Yip, D. Mazziotti, and H. Rabitz, J. Chem. Phys. 118, 8168-8172(2003).

[14] H. Rabitz, M. Hsieh and C. Rosenthal, Science, 303, 1998-2001 (2004)

[15] H. Rabitz, C. L. Bris and G. Turinici, to appear in Phys. Rev. E.

[16] V. Ramakrishna, M. V. Salapaka, M. Dahleh, H. Rabitz and A. Peirce, Phys. Rev. A., 51, 960-966, (1995)

[17] V. Jurdjevic and H. Sussmann, J. of Differential Equations, 12, 313-329, (1972)

[18] F. Ayres. Jr., Theory and Problems of Matrices, New York: Schaum, p. 181, (1962)

[19] G. Turinici and H. Rabitz, Chem. Phys., 267, 1-9, (2001)

[20] G. Turinici, http://www-rocq.inria.fr/Gabriel.Turnici/control/criterion.html

[21] A. Mitra and H. Rabitz, Phys. Rev. A., 67, 033407-1-16, (2003)

[22] L. Gonzalez, D. Kroner, and I. R. Sola, J. Chem. Phys., 115, 2519-2529, (2001)

[23] L. Gonzalez, K. Hoki, D. Kroner, A. S. Leal, J. Manz, and Y. Ohtsuki, J. Chem. Phys., 113, 11134-11142, (2002)

[24] Y. Fujimura, L. Gonzalez, D. Kroner, J. Manz, I. Mehdaoui, and B. Schmidt, Chem. Phys. Lett., 386, 248-253 (2004)

[25] R. Wu, I. Solá and H. Rabitz, submitted.

[26] R. Diestel, Graph Theory, Springer-Verlag New York, 2000

[27] Z. Amitay, R. Kosloff, S. R. Leone, Chem. Phys. Lett., 359, 8-14 (2002)

[28] Given a sequence of probability spaces, let q_n be the probability that property Q holds in

the nth space. Probability Q *almost always* holds if $lim_{n\to\infty} q_n = 1$. Here, the nth space is a probability distribution over n-vertex graphs. D. B. West, Introduction to Graph Theory, Prentice Hall, p. 430, 2001.

[29] For $N = 30$, there are 435 pairs of states. Thus, the possible values for the fraction of connected pairs of states are $0/435, 1/435, 2/435, 3/435, \ldots, 434/435$ and $435/435$. However, the discretization level shown in Fig.3 evidently is even more sparse than this inherent discreteness.